Enhanced absorption in heterostructure composed of graphene and a doped photonic crystal

YONGQIANG KANG[a,b], HONGMEI LIU[a,*], QIZHI CAO[c,*]
[a]*Institute of solid state physics, Shanxi Datong University, Datong, Shanxi 037009, China*
[b]*Xi'an mengxibitan information technology limited company, Shaanxi 710049, China*
[c]*School of Physics and Electronic Information Science, Guangxi Teachers Education University, Nanning 530023, China*

The optical absorption in heterostructure composed of a graphene and a doped photonic crystal is investigated theoretically. The absorption of the heterostructure is enhanced greatly due to photon localization. The absorptance can be tuned by varying either the incident angle or the thickness of graphene film. The number of absorption peaks can be tuned by varying the thickness of dielectric defect.

(Received January 16, 2018; accepted November 29, 2018)

Keywords: Absorption, Graphene, A doped photonic crystal

1. Introduction

Graphene is currently the subject of intense research in both theoretical and experimental sides. The interest is driven by its unique electrical and optical properties [1-8]. These properties led to numerous important applications in optoelectronic and nanophotonic devices such as transparent electrodes, ultrafast lasers, polarizers, and photodetectors. A unique optical property of graphene is that its absorption is nearly constant over the visible and near- infrared regions [9-12].

Although graphene exhibits almost uniform absorption within a large wavelength range, its optical absorption in graphene is minimal, which is detrimental to the fabrication of some optoelectronic devices, such as the optical detectors. Therefore, various approaches have been proposed to enhance the absorption of graphene, including using exciting plasmons in doped graphene nanostructures, combining graphene-based one-dimensional photonic crystals(PCs) containing a x-cut lithium niobate layer [4], graphene-based hybrid nanostructure cavity [5], forming periodically patterned graphene, and integrating graphene with microcavities [13-20]. In this context, the enhanced absorption of some two-dimensional materials, such as, black phosphorus, hBN have been reported [13-16]. Besides, multilayer graphene structures can also hold unusual optical response owing to the interaction of charge carriers with the electromagnetic waves in the different layers. Nevertheless, few works have been dedicated to the study of optical absorption enhancement in heterostructure composed of a graphene and a doped photonic crystal. Compared with the previously reported methods to enhance the absorption of graphene using nanostructures or by putting graphene in microcavities, it is relatively easy to prepare graphene films on the top of bulk materials or one dimensional photoic crystal [20].

In the present paper, we theoretically investigate the optical absorption in heterostructure composed of a graphene and a doped photonic crystal. We deposit monolayer, two graphene layer and three graphene layer on the top of doped photonic crystal (the interaction between layers is ignored when the number of graphene layers increased). The absorptance of graphene film on one dimension photionic crystal with defect is enhanced greatly duo to photon localization. The absorptance can be tuned by varying either the incident angle or the thickness of graphene film. The number of absorption peaks can be tuned by varying the thickness of dielectric defect.

2. Absorption of a doped photonic crystal

A doped photonic crystal structure denoted $(BC)^4D(BC)^4$, $B(C)$ and D represent the high(low)-refractive-index materials and defect layer, respectively. Their refractive indices are described by $n_j = n_{rj} + k_j i,\ j = B, C, D$, in which $n_{rj}(k_j)$ is the real (imaginary) part of the refractive index. Because the imaginary part of the refractive index is proportional to the absorption coefficient, we define k_j as the absorption coefficient of the materials in this paper. The thicknesses of *B*, *C*, and *D* are denoted d_B, d_C, and d_D, respectively. The periodic number of the structure is *N*. In our calculations, we choose $n_{rB} = n_{rD} = 3.5$, $n_{rC} = 1.456$, $k_B = k_C = 0.00007$, $d_C = 80\text{nm}$ [21]. The optical

thicknesses of B and C are assumed to satisfy $n_{rB}d_B = n_{rC}d_C$. The thickness of the defect layer is $d_D = 3.141d_B$. In this paper, the transfer matrix method [22-24] is used to calculate the transmittance (T) and reflectance (R) of the heterostructure, and their absorptance (A) as follows:

$$R = |r|^2 = \left| \frac{m_{11}\eta_0 + m_{12}\eta_0\eta_{n+1} - m_{21} - m_{22}\eta_0}{m_{11}\eta_0 + m_{12}\eta_0\eta_{n+1} + m_{21} + m_{22}\eta_0} \right|^2 \quad (1)$$

$$\mathrm{T} = |t|^2 = \left| \frac{2\eta_0}{m_{11}\eta_0 + m_{12}\eta_0\eta_{n+1} + m_{21} + m_{22}\eta_0} \right| \quad (2)$$

$$A = 1 - T - R \quad (3)$$

where $\eta_j = \sqrt{\varepsilon_j}\Big/\sqrt{\mu_j}\sqrt{1-\sin^2\theta/\varepsilon_j\mu_j}$ for TE polarization, and $\eta_j = \sqrt{\mu_j}\Big/\sqrt{\varepsilon_j}\sqrt{1-\sin^2\theta/\varepsilon_j\mu_j}$ for TM polarization. η_0 and η_{n+1} are the incident and exit media for the corresponding η parameter, respectively. m_{11}, m_{12}, m_{21}, and m_{22} are the elements of total transfer matrix.

$$\mathrm{M} = \begin{pmatrix} \cos(k_z^j d_i) & -\dfrac{i}{\eta_j}\sin(k_z^j d_j) \\ i\eta_j \sin(k_z^j d_j) & \cos(k_z^j d_j) \end{pmatrix}, \quad (4)$$

where $k_z^j = \omega/c\sqrt{\varepsilon_j\mu_j}\cos\theta_j$ is the z component of the wave vector. θ_j is the ray angle in jth layer which is related to the Snell's law of refraction.

Fig. 1 shows the absorption of the structure $(BC)^4D(BC)^4$ as a function of absorption coefficient k_D and wavelength λ for normal incidence. One can see that the absorbance of the defect mode is nonmonotonic and reaches a maximum at k_D=0.005 with increasing the absorption coefficient k_D. This result conflicts with the conventional viewpoint that the absorption of defect mode will be enhanced with increasing the absorption coefficient of the defect. The reason is that the absorption coefficient of the defect increasing results in an impedance mismatch at entrance face of the structure, which leads to stronger reflectance. In other word, fewer EM waves of the defect mode will enter the structure. So the absorbance decreases when the defect layer has a larger absorption coefficient. Therefore, it is impossible to enhance absorbance by increasing the absorption coefficient of defect for photonic crystal with a lossy dielectric defect.

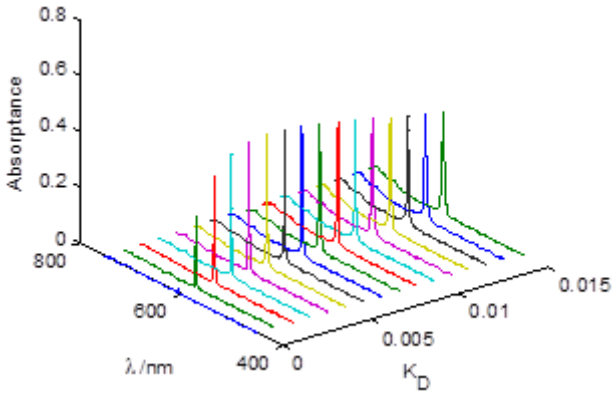

Fig. 1. The absorption of the structure $(BC)^4D(BC)^4$ as a function of absorption coefficient K_D and wavelength λ for normal incidence, B(C) and D represent the high(low)-refractive-index materials and defect layer, respective

3. Enhance absorption with graphene

To let all of the light of defect mode enter the structure and make the absorption enhancement, a heterostructure $G(BC)^ND(BC)^N$ is employing, where G and $(BC)^ND(BC)^N$ represent the graphene film and a doped photonic crystal, respectively. Graphene is described by the wavelength-dependent complex refractive index $n(\lambda) = 3.0 + C_1\lambda/3i\,(C_1 = 5.446um^{-1})$ in the visible range [6,20], and the thickness of a graphene monolayer is 0.34 nm. It is considered here are composed of a graphene film and one dimensional photonic crystal with defect, as shown in Fig. 2.

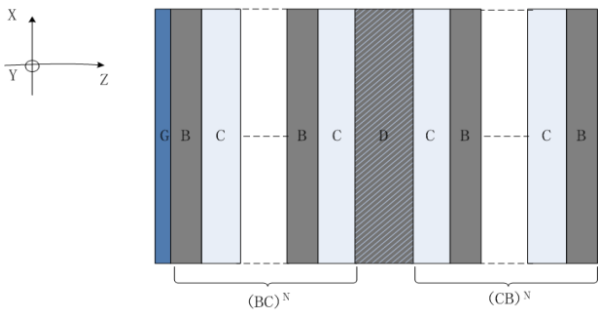

Fig. 2. (Color online) Schematic diagram of a heterostructure $G(BC)^ND(CB)^N$ composed of a graphene film G and doped photonic crystal $(BC)^ND(CB)^N$. N is total period number

For normal incidence, the optical absorption spectra of the heterostructure $G(BC)^N D(BC)^N$ without and with the graphene films of different thickness are shown in Fig. 3, where G_1, G_2 and G_3 denote monolayer, two layer and three graphene, respectively(the interaction between layers is ignored when the number of graphene layers increased). The absorption coefficient of the defect layer is $k_D = 0.004$. It can be seen that the optical absorption of graphene monolayer is about 2.3% and independent of the wavelength in the visible wavelength region (see black dashed line in Fig. 3). This is consistent with refer. 20. The optical absorption of the doped photonic crystal $(BC)^N D(BC)^N$ without graphene films is about 28.5% (see blue dotted line in Fig. 3). In contrast, when a graphene monolayer is prepared on top of the doped photonic crystal, the maximum absorption is about 31.8%and the absorption peak appears at 612 nm (see green solid line in Fig. 3). Moreover, as the layer number of graphene increases, its absorption becomes stronger. Three graphene layers can achieve an absorptance of about 37.6% (see red solid line in Fig. 3). It is about 16 times larger than that of the graphene monolayer without the doped photonic crystals.

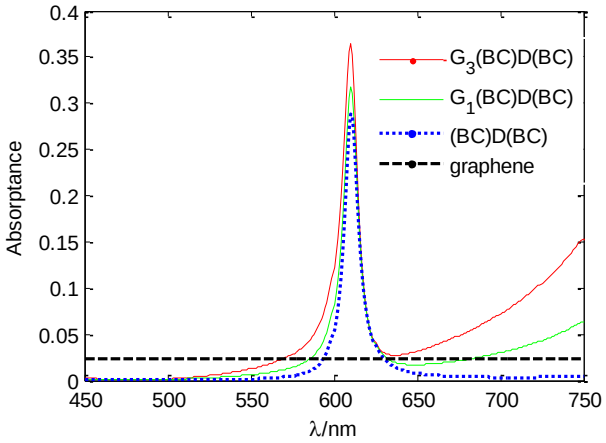

Fig. 3. The absorptance of graphene as a function of light wavelength for heterostructures with and without graphene layer at normal incidence: single graphene (black dashed line), heterostructures without graphene layer(blue dotted line), heterostructures with single graphene layer (red solid line) heterostructures with three graphene layer (green solid line)

To reveal the physical origin of the enhanced absorption in heterostructures containing graphene, we numerically calculated the magnetic fields intensity distribution $|H|$ for the heterostructure $G(BC)^N D(BC)^N$ with a graphene monolayer and the doped photonic crystal $(BC)^N D(CB)^N$ at $\lambda = 612$ nm. The results are presented in Fig. 4. The thickness of the graphene monolayer in the schematic diagram is 100 times its actual thickness, as shown in Fig. 4(a). One can see that there are strong localized magnetic fields between the interface of the graphene and the heterostructure $(BC)^4 D(BC)^4$ within the dielectric defect layer at the wavelength $\lambda = 612$ nm, which greatly enhances the absorption. This is because the coupling effect can realize stronger localized EM field in $G(BC)^N D(BC)^N$ than in $(BC)^N D(BC)^N$ to enhance absorption. Without the graphene film, the absorbance of defect mode for the structure $(BC)^N D(BC)^N$ is 28.5%, as shown blue dotted line by Fig. 3. The reason is that there are still strong localized EM fields within the defect layer, as shown in Fig. 4(b)

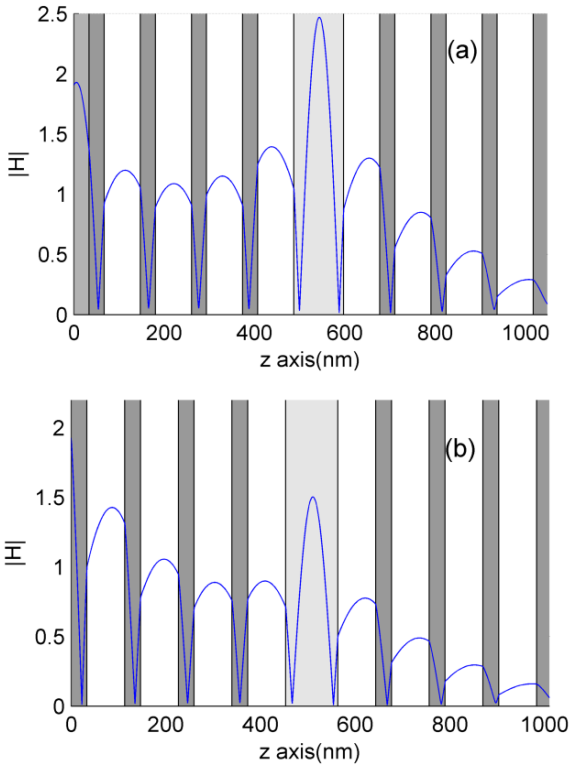

Fig. 4. The magnetic fields intensity at $\lambda = 612$ nm (a) the heterostructures composed of a graphene film G and the doped photonic crystal $(BC)^N D(CB)^N$,(b) the doped photonic crystal $(BC)^N D(CB)^N$

4. The effect of incident angle

Moreover, the oblique incidence of light was considered for both transverse electric (TE) and transverse magnetic (TM) polarizations. Fig. 5 display the absorption spectra of the heterostructure $G(BC)^N D(BC)^N$ for TE and TM waves at oblique incidence. It can be seen that the absorption peak moves toward shorter wavelengths with increasing incident angle for both TE and TM modes. For the TE mode, when incident angle θ increases, the absorption is enhanced. For example, the absorptance of a graphene monolayer (three graphene layer) can be about 39.2% (41.7%) at $\theta = 60^\circ$, and the center wavelength of

the absorption peak is about 591 nm (see blue dotted line in Figs. 5(a) and 5(b)). The feature is fully consistent with light propagation in an optical micro-cavity. The resonance condition of a micro-cavity can be described as $2L_o k_z = 2m\pi$, where m is an integers. L_o is optical path of the spacer layer, $k_z = k\cos\theta$, k is the wave vector of light, and θ is the propagation angle of light in spacer layer, leading to a resonant wavelength in micro-cavity of $\lambda \propto \cos\theta$ [20].

In the TM mode, as the incident angle increases, the absorption of the heterostructure $G(BC)^N D(BC)^N$ is reduced. For example, the absorptance of a graphene monolayer and three layer graphene with heterostructures are about 20% and 26% at $\theta = 60°$, respectively.(see blue dotted line in Figs. 5(c) and 5(d)). The reason is that the electric field component is no longer parallel to the graphene sheet for TM mode, the absorption of graphene is reduced.

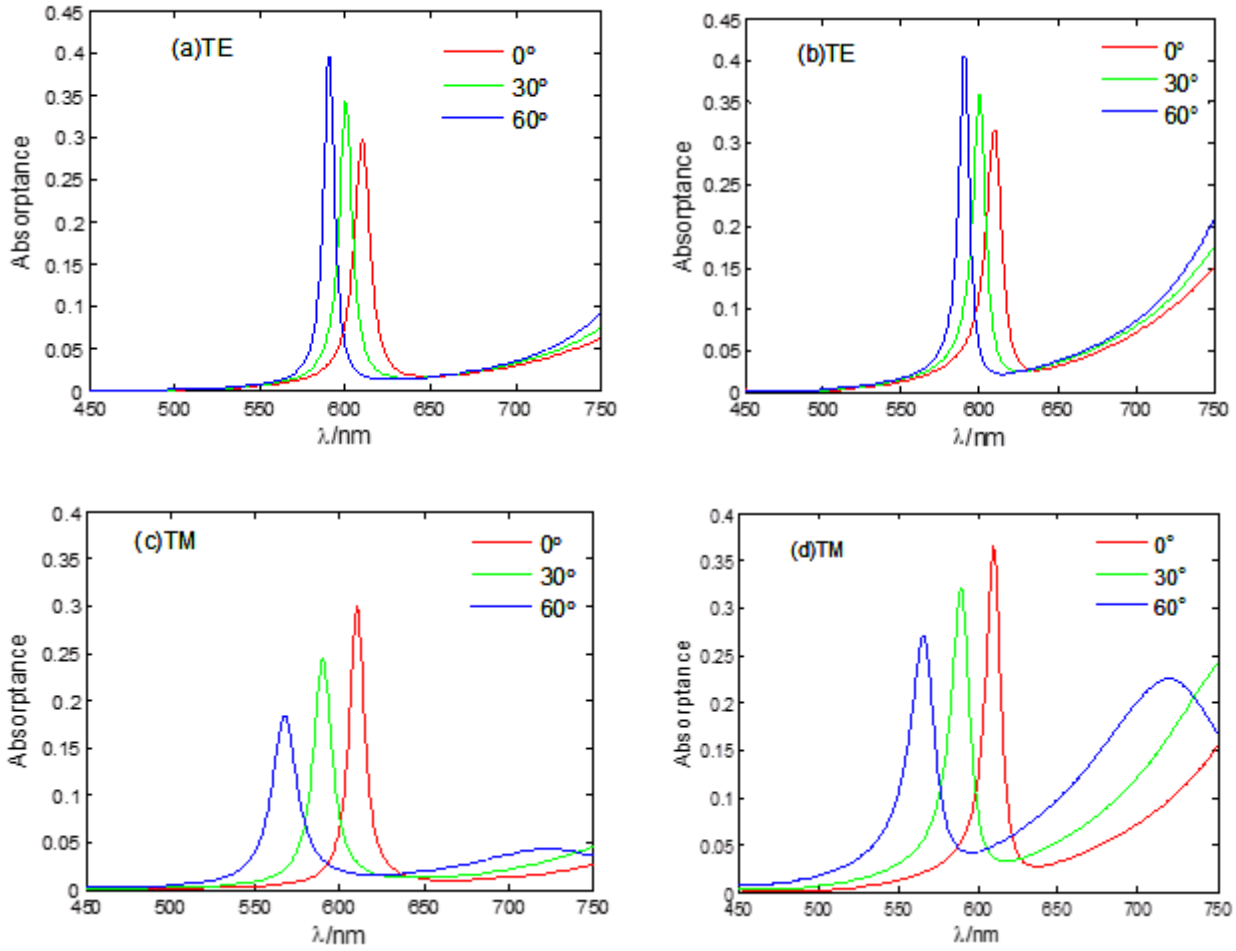

Fig. 5. The absorptance of graphene on doped photonic crystal $(BC)^N D(CB)^N$ as a function of the light wavelength for different incident angles:(a) the graphene monolayer for TE, (b) the three graphene layer for TE, (c) the graphene monolayer for TM, (d) the three graphene layer for TM

5. The effect of thickness of dielectric

Finally, the number of absorption peaks can be tuned by varying the thickness of dielectric defect of the heterostructure. Fig. 6(a)-6(d) correspond to d_D=104 nm, 312 nm, 416 nm and 520 nm, respectively. We can see that absorption peak is split into, two, three and four as the thickness of defect increases. The larger the thickness value is, the more absorption peaks are formed. The splitting of the absorption peak can be explained by using the tight-binding approach [25-27]. Hence we can generate as many absorption peaks as desired simply by adjusting the thickness of dielectric defect. This feather is of technical importance because these absorption peaks can be used as the fabrication of some optoelectronic devices, such as the optical detectors.

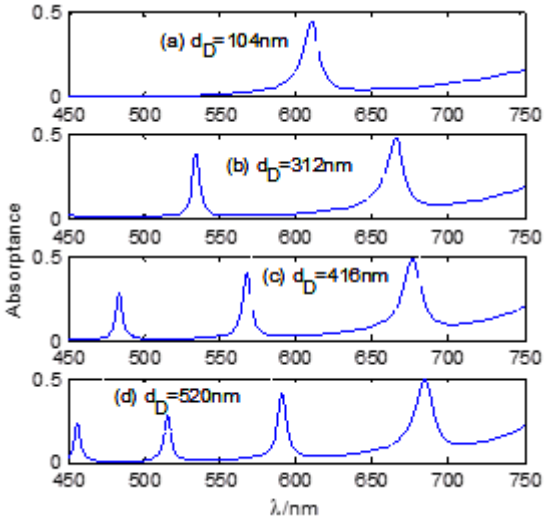

Fig. 6. The absorptance of graphene on doped photonic crystal $(BC)^N D(CB)^N$ as a function of the light wavelength for different thickness of dielectric defect at normal incidence: (a) d_D = 104 nm, (b) d_D = 312 nm, (c) d_D=416 nm (d) d_D=520 nm

6. Conclusion

In summary, we investigated the optical absorption of graphene layer prepared on the top of a doped photonic crystal theoretically. It is found that the absorption of graphene on heterostructure can be enhanced by about sixteen times under normal incidence light. The absorptance of the heterostructure can be tuned by varying incident angle and thickness of graphene. The number of absorption peaks can be tuned by varying the thickness of dielectric defect. Our proposal is very easy to implement using the existing technology and may have potentially important applications in optoelectronic devices.

Acknowledgement

This research was financially supported by the National Science Foundation for China (Grant NO.11664004) and Launching Scientific Research Funds for Doctors (Grant NO.2014-B-04) and Shanxi Provincial Science Foundation (Grant NO. 201601D021029) and Science and Technology Project of Datong City (NO.2017131) and Natural Science Foundation of Guangxi Province (2016GXNSFAA380241).

References

[1] W. D. Tan, C. Y. Su, R. J. Knize, G. Q. Xie, Appl. Phys. Lett. **96**(3), 031106-3 (2010).
[2] Q. Bao, H. Zhang, B. Wang, Z. Ni, C. H. Y. X. Lim, Y. Wang, et al., Nat. Photo. **5**(7), 411 (2011).
[3] Z. Fang, Z. Liu, Y. Wang, P. M. Ajayan, P. Nordlander, N. J. Halas, Nano Lett. **12**(7), 3808 (2012).
[4] A. Rashidi, A. Namdar, R. Abdi-Ghaleh, Superlattices & Microstructures **105**, 74 (2017).
[5] A. Rashidi, A. Namdar, European Physical Journal B **91**(4), 68 (2018).
[6] R. Miloua, Z. Kebbab, F. Chiker, M. Khadraoui, K. Sahraoui, A. Bouzidi, et al., Optics Communications **330**, 135 (2014).
[7] X. K. Kong, X. Z. Shi, J. J. Mo, Y. T. Fang, X. L. Chen, S. B. Liu, Optics Communications **383**, 391 (2017).
[8] Y. Xiang, X. Dai, J. Guo, H. Zhang, S. Wen, D. Tang, Sci. Rep. **4**, 5483 (2014).
[9] J. Guo, L. Wu, X. Dai, Y. Xiang, D. Fan, AIP Advances **7**(2), 025101 (2017).
[10] J. Wu, L. Jiang, J. Guo, X. Dai, Y. Xiang, S. Wen, Optics Express **24**(15), 17103 (2016).
[11] Q. Ye, J. Wang, Z. Liu, Z. C. Deng, X. T. Kong, F. Xing, et al., Appl. Phys. Lett. **102**(2), 021912 (2013).
[12] K. F. Mak, L. Ju, F. Wang, T. F. Heinz, Solid State Commun. **152**(15), 1341 (2012).
[13] J. Wu, H. Wang, L. Jiang, J. Guo, X. Dai, Y. Xiang, et al., Journal of Applied P hysics **119**(20), 74 (2016).
[14] J. Wu, J. Guo, X. Wang, L. Liang, X. Dai, Y. Xiang, et al., Plasmonics **13**(3), 803 (2018).
[15] X. Wang, Q. Ma, L. Wu, J. Guo, S. Lu, X. Xai, et al., Optics Express **26**(5), 5488 (2018).
[16] H. Xu, J. Guo, L. Wu, X. Dai, Y. Xiang, Photonics Research **4**(6), 262 (2016).
[17] X. Zhu, L. Shi, M. S. Schmidt, A. Boisen, O. Hansen, J. Zi, et al., Nano. Lett. **13**(10), 4690 (2013).
[18] X. Gan, K. F. Mak, Y. Gao, Y. You, F. Hatami, J. Hone, et al., Nano. Lett. **12**(11), 5626 (2012).
[19] A. Ferreira, N. M. R. Peres, R. M. Ribeiro, T. Stauber, Phys. Rev. B **85**(11), (2012).
[20] J. T. Liu, N. H. Liu, J. Li, Jing X. Li, J. H. Huang, Appl. Phys. Lett. **101**(5), 052104 (2012).
[21] Z. Zhang, G. Du, H. Jiang, Y. Li, Z. Wang, H. Chen, J. Opt. Soc. Am. B **27**(5), 909 (2010).
[22] Y. Kang, H. Liu, Q. Cao, Optical Engineering **57**(3), 037102 (2018).
[23] Y. Kang, H. Liu, Superlattices & Microstructures **114**, 355 (2018).
[24] Y. Xiang, X. Dai, S. Wen, D. Fan, J. Opt. Soc. Am. A **24**(10), 28 (2007).
[25] Y. H. Chen, S. Varma, H. M. Milchberg, J. Opt. Soc. Am. B **25**(7), B122 (2008).
[26] H. Jiang, H. Chen, H. Li, Y. Zhang, J. Zi, S. Zhu, Phys. Rev. E **69**(2), 066607 (2004).
[27] Q. Qin, H. Lu, S. N. Zhu, C. S. Yuan, Y. Y. Zhu, N. B. Ming, Appl. Phys. Lett. **82**(26), 4654 (2003).

*Corresponding author: lhm9898@163.com;
qzhcao77@163.com;
kyq_2000@sohu.com